

# Segmentation of Retinal Cysts in OCT Images

Fauzi .

Student ID : 250286733

Module : Image Processing (CSC8628)

November 13, 2025

## Contents

<b>1</b>	<b>Introduction</b>	<b>3</b>
1.1	Overview .....	3
1.2	Clinical Significance and Challenges .....	3
1.3	Relevant Literature .....	3
<b>2</b>	<b>Methodology</b>	<b>4</b>
2.1	Proposed Algorithm .....	4
2.2	Workflow Diagram .....	6
<b>3</b>	<b>Implementation Details</b>	<b>8</b>
3.1	Libraries, Frameworks, and Functions .....	8
3.2	Justification .....	8
<b>4</b>	<b>Results</b>	<b>9</b>
4.1	Quantitative Metrics .....	9
4.2	Qualitative Visualizations .....	9
<b>5</b>	<b>Discussion</b>	<b>11</b>
<b>6</b>	<b>Conclusions</b>	<b>12</b>
6.1	Summary .....	12
6.2	Future Work .....	12
	<b>References</b>	<b>12</b>

# **1 Introduction**

## **1.1 Overview**

Optical Coherence Tomography (OCT) retinal images are used by ophthalmologists to identify eye health by analysing the structure beneath the eye. The retina is scanned using light waves to take cross sectional images with OCT. With OCT image analysis, some retinal diseases can be identified, including retinal cysts. Moreover, retinal cyst detection is an important diagnostic sign that can be associated with primary diseases, such as Diabetic Macular Oedema and Diabetic Retinopathy.

## **1.2 Clinical Significance and Challenges**

The large number of captured images becomes the main issue, as cyst identification by the expert does not occur quickly. Furthermore, manual or qualitative segmentation analysis often relies on human interpretation, which leads to subjectivity and inconsistency. This work aims to develop algorithms that can automatically segment retinal cysts in OCT retinal images. However, the cyst segmentation task faces challenges due to the variety of different types of OCT scans. Some images might have a different orientation and level of noise. Moreover, variety in size, shape and intensity of the cyst presents another challenge.

## **1.3 Relevant Literature**

Several relevant studies on the development of algorithms for image segmentation and detection explain the use of filters, morphological operations, and Region of Interest (ROI) techniques. A study by Hafeez et al. (2023) explains that the use of morphological operators is helpful in detecting boundaries and sharpening the region of the image. In this case, morphological operators were used to identify brain tumours. This paper also applies median filters to remove noise.

In addition, traditional methods employ Region of Interest (ROI) techniques for localised segmentation, which helps isolate cystic structures in retinal layers (Gopinath & Sivaswamy, 2019). Gopinath and Sivaswamy highlighted that the vital task in the segmentation issue is the localisation of the region of interest. Therefore, the region of interest can be extracted in preprocessing and used for further processing.

## 2 Methodology

### 2.1 Proposed Algorithm

The proposed algorithm comprises three main stages: preprocessing, segmentation, and postprocessing.

#### 1. Preprocessing

##### a. Denoising

Denoising was applied to the first branch of preprocessing. For OCT scan image processing, denoising is an important step, which helps to reduce noise due to image acquisition. In this work, we selected two nonlinear filters, the morphological opening and the median filter. The denoised image will be used as input for generating the Retinal Region of Interest (ROI). The result is shown in Figure 1c.

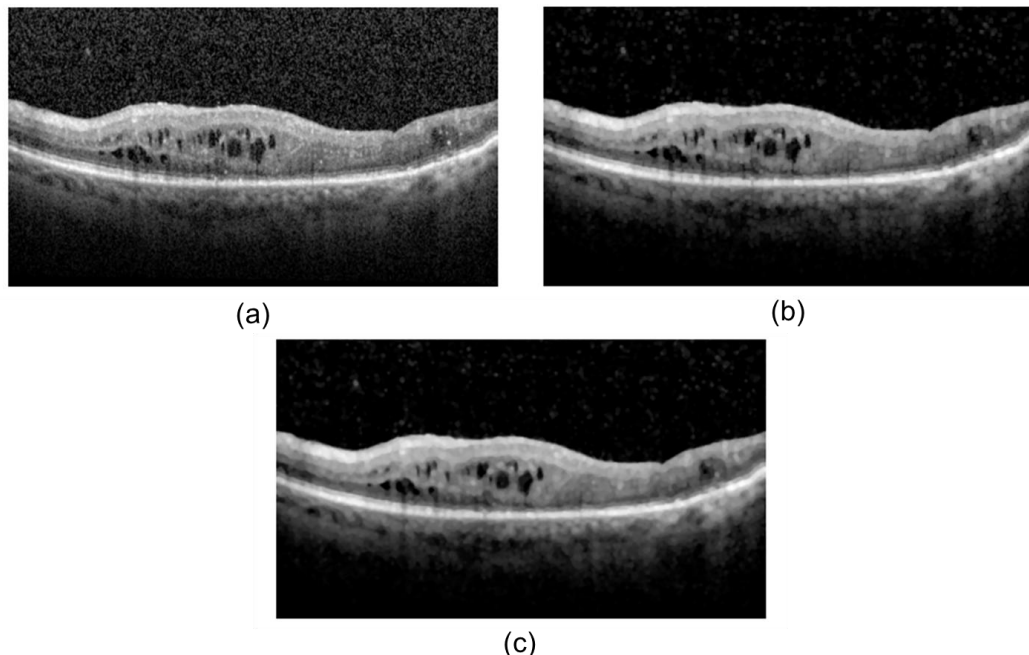


**Figure 1:** Denoising step. (a) Original Image, (b) Morphological Opening, and (c) Median Filter.

##### b. Enhancing

For the second branch of preprocessing, image enhancement was applied to sharpen the image's edges and enhance the black and white colours by increasing image contrast and adjusting image highlights and shadows. Image's edges were noticeable after applying this enhancement step. The result would be used in a further step for cyst feature segmentation.

#### 2. Segmentation

##### a. Retinal Region of Interest (RoI)

Cysts are located within layers between the Internal Limiting Membrane (ILM) and the Retinal Pigment Epithelium (RPE) (Gopinath & Sivaswamy, 2019), both of which are illustrated in Figure 2. Segmentation of the retinal Region of Interest (RoI) is proposed using Otsu method and Morphological Closing. In detail, to get a better ILM edge, we applied Otsu method and then morphological closing using a small kernel ( $5 \times 5$ ). A small kernel was necessary to trace the top boundary accurately, especially at the fovea. The output image was named top RoI.

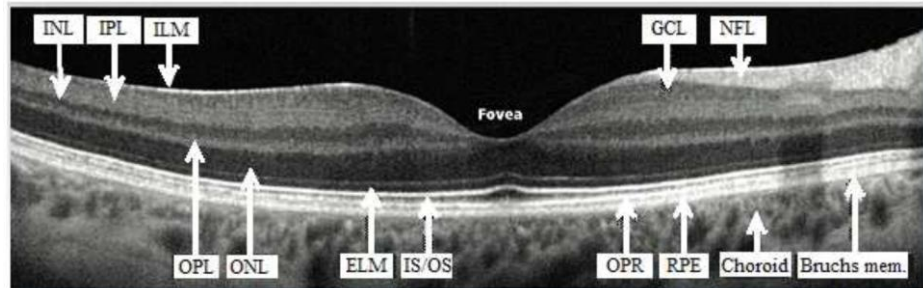


**Figure 2:** Optical coherence tomography of retina showing layer names, including Inner limiting membrane (ILM) and Retinal Pigment Epithelium (RPE) (Ravichandran et al., 2019).

On the other hand, for the bottom boundary, Otsu threshold segmentation was applied to the OCT scan, followed by morphological closing with a large kernel ( $60 \times 60$ ) to create a solid retinal base. The output image was named bottom RoI. The next step in retinal RoI segmentation was to mask the top RoI and bottom RoI using the bitwise operation. We selected the bitwise AND operator to extract regions of interest between the ILM and RPE from OCT images, using the top RoI and bottom RoI masks. This mask was refined using a median filter, morphological opening, and closing to obtain the final retinal RoI mask (Figure 3e).

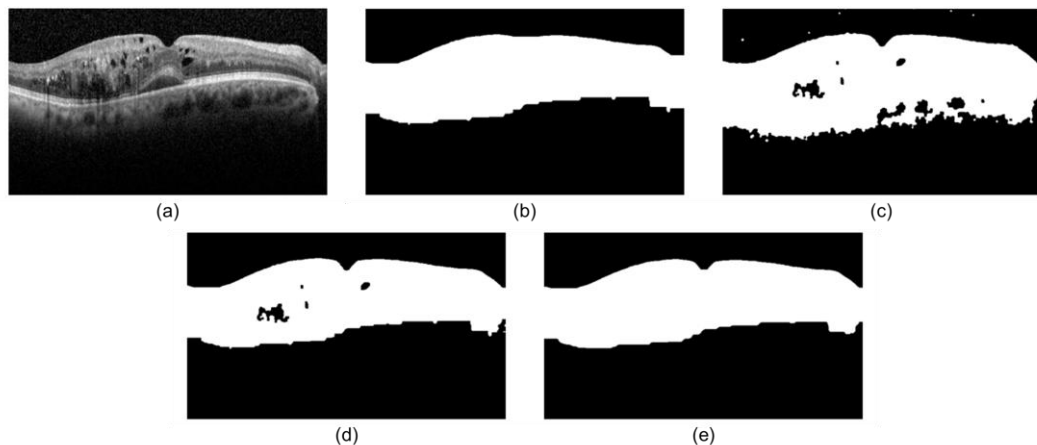


**Figure 3:** Results of Retinal Region of Interest Extraction. (a) Original Image, (b) Bottom RoI Mask, (c) Top RoI Mask, (d) Combined Mask, and (e) Final RoI Mask.

### b. Cyst Feature Segmentation

Cyst feature segmentation becomes the primary step in the segmentation process. The image generated from preprocessing 1b was segmented using a K-means clustering. The cluster was set to 4, which means the algorithm would identify and group pixels with similar colours into 4 clusters (Figure 4b). This number of clusters performed the best result compared to other numbers.

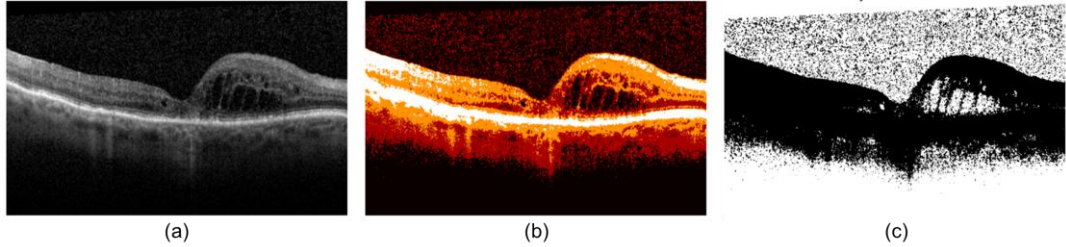


**Figure 4:** Visualising the K-means Segmentation Process. (a) Original Image, (b) K-means Clusters, (c) Selected Darkest Cluster (Cysts).

### c. Final Prediction (Masking)

The final prediction image was generated by combining the final ROI mask and the result image from the cyst feature segmentation step. We employed the bitwise AND operator to retain the white in cysts and remove the area above the ILM and below the RPE. The possible cysts, indicated by white pixels within the retina, would be retained in this process.

## 3. Postprocessing

For postprocessing, we applied only one type of filter, the morphological closing filter. A morphological closing filter was applied to remove small black points within the potential cysts. We used a  $3 \times 3$  kernel size for the morphological filter. We did not apply any other filter or combine it with other nonlinear filters, as this would decrease the mIoU score.

## 2.2 Workflow Diagram

The complete workflow of the proposed algorithm is illustrated in Figure 5.

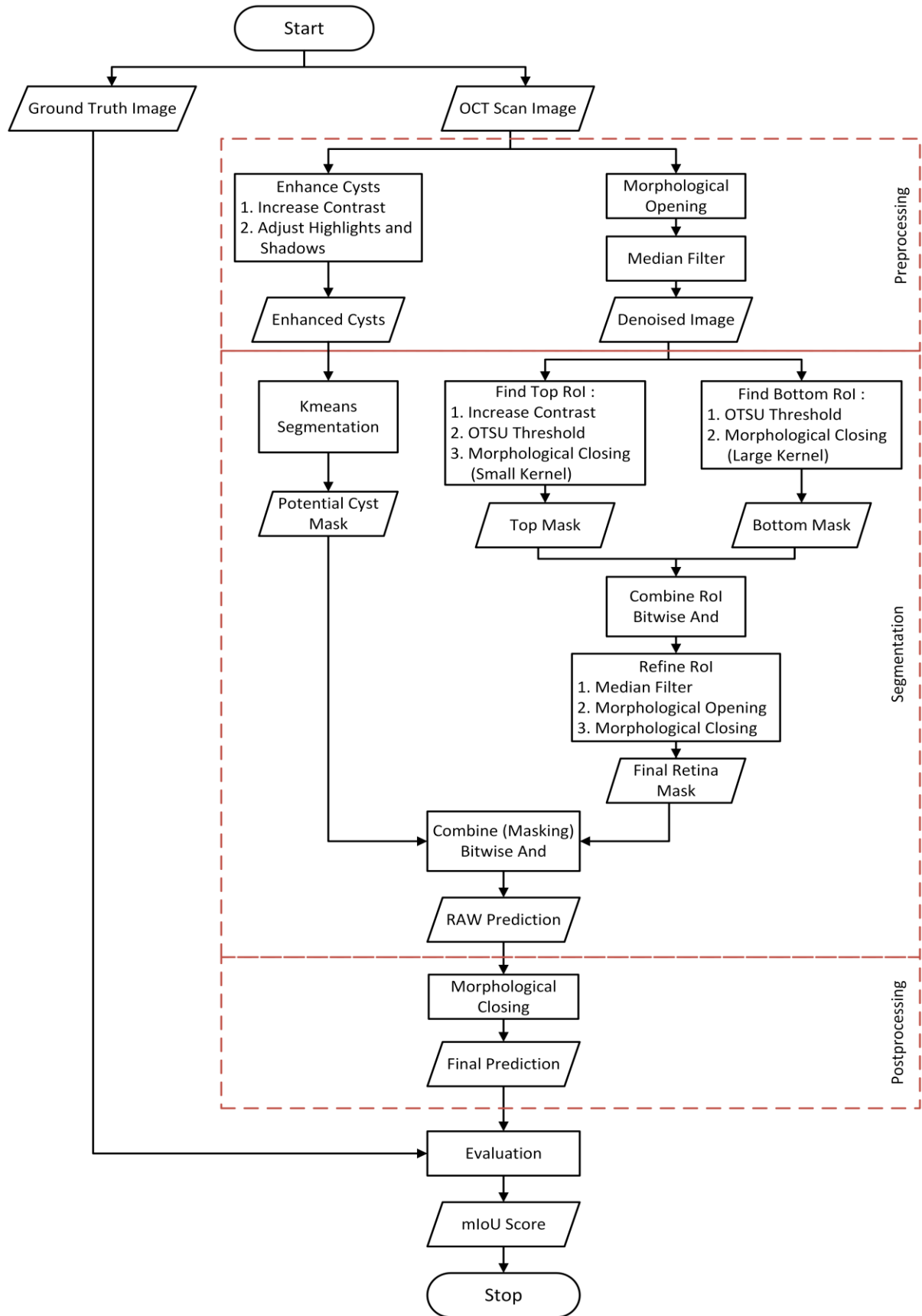


**Figure 5:** The complete workflow of data processing and segmentation.

### 3 Implementation Details

#### 3.1 Libraries, Frameworks, and Functions

The algorithm was implemented in Python (v3.13.3). The core functionality relies on several key opensource libraries, which are summarised in Table 1.

**Table 1:** Summary of Python Libraries and Their Roles in the Work.

Library	Role in Work	Key Functions Used
OpenCV (cv2)	Core Image Processing	imread morphologyEx medianBlur kmeans threshold (otsu & inv) bitwise_and
NumPy (np)	Numerical Array Manipulation	array flatten astype clip ones
Matplotlib	Qualitative Visualisation & Debugging	pyplot.imshow pyplot.subplot pyplot.title pyplot.figure
OS	File System Automation	listdir
Sklearn.metrics	Quantitative Metric Evaluation	jaccard_score f1_score precision_score recall_score accuracy_score
Time	Performance Benchmarking	time
Statistics	Metric Consistency Analysis	stdev

#### 3.2 Justification

- **OpenCV** was chosen as the primary image processing framework due to its high speed, C++ backed operations. Since the pipeline involves multiple morphological and filtering steps on each image, OpenCV's performance was essential.
- **Scikit-learn** was chosen for all evaluation metrics because it provides standardised, community-verified implementations of the Jaccard score, F1 score, etc. This ensures that the results are accurate, reliable, and comparable to other papers.
- **Matplotlib and Numpy** were chosen for output visualisation of each pipeline stage and kernel creation.
- **Time and statistics** were added to provide a complete performance profile, measuring not only the accuracy but also the speed and consistency of the algorithm.

## 4 Results

The proposed pipeline was implemented on a Radeon 880M GPU, with 24GB of RAM on a Ryzen AI 9 365 processor. The proposed algorithm was tested on the provided OCT dataset. The OCT dataset has 10 original and 10 annotation images.

### 4.1 Quantitative Metrics

The segmentation performance was evaluated using six key metrics: Processing Time (in seconds), mIoU Score, Accuracy, Precision, Recall, and F1 Score. The full performance metrics for each image are presented in Table 2. A summary of the average performance metric is shown in Table 3. The detailed examination of the evaluation metrics in Table 4 provides important insights into the performance of the K-means approach compared to other methods, such as the Manual threshold and the Otsu method.

**Table 2:** Evaluation Metrics Table.

Metric	Image									
	1	2	3	4	5	6	7	8	9	10
Proc time	0.130	0.124	0.135	0.093	0.136	0.133	0.133	0.149	0.135	0.143
mIoU score	0.172	0.429	0.659	0.256	0.434	0.636	0.391	0.197	0.193	0.128
Accuracy	0.987	0.994	0.992	0.982	0.984	0.995	0.982	0.983	0.983	0.984
Precision	0.240	0.701	0.725	0.362	0.501	0.823	0.506	0.702	0.23	0.393
Recall	0.377	0.526	0.879	0.466	0.766	0.737	0.632	0.216	0.543	0.160
F1 score	0.293	0.601	0.795	0.408	0.606	0.778	0.562	0.330	0.323	0.227

**Tabel 3:** Overall Average Metrics.

Metric	Average	Std Dev
Processing time (sec)	0.131	0.015
mIoU score	0.350	0.192
Accuracy	0.986	0.005
Precision	0.518	0.212
Recall	0.530	0.234
F1 score	0.492	0.204

**Tabel 4:** Performance evaluation metrics for the K-means segmentation approach compared to other methods (Manual Threshold and Otsu).

Segmentation Approach	Evaluation Metrics					
	Proc Time	mIoU Score	Accuracy	Precision	Recall	F1 score
K-means	0.131	0.350	0.986	0.518	0.530	0.492
Manual Threshold	0.010	0.306	0.977	0.359	0.713	0.458
Otsu	0.010	0.141	0.922	0.142	0.955	0.245

## 4.2 Qualitative Visualisations

The qualitative segmentation results are presented in Figure 6. This figure provides a visual comparison between the original OCT image, its corresponding ground truth, and the final segmentation mask produced by the proposed algorithm.

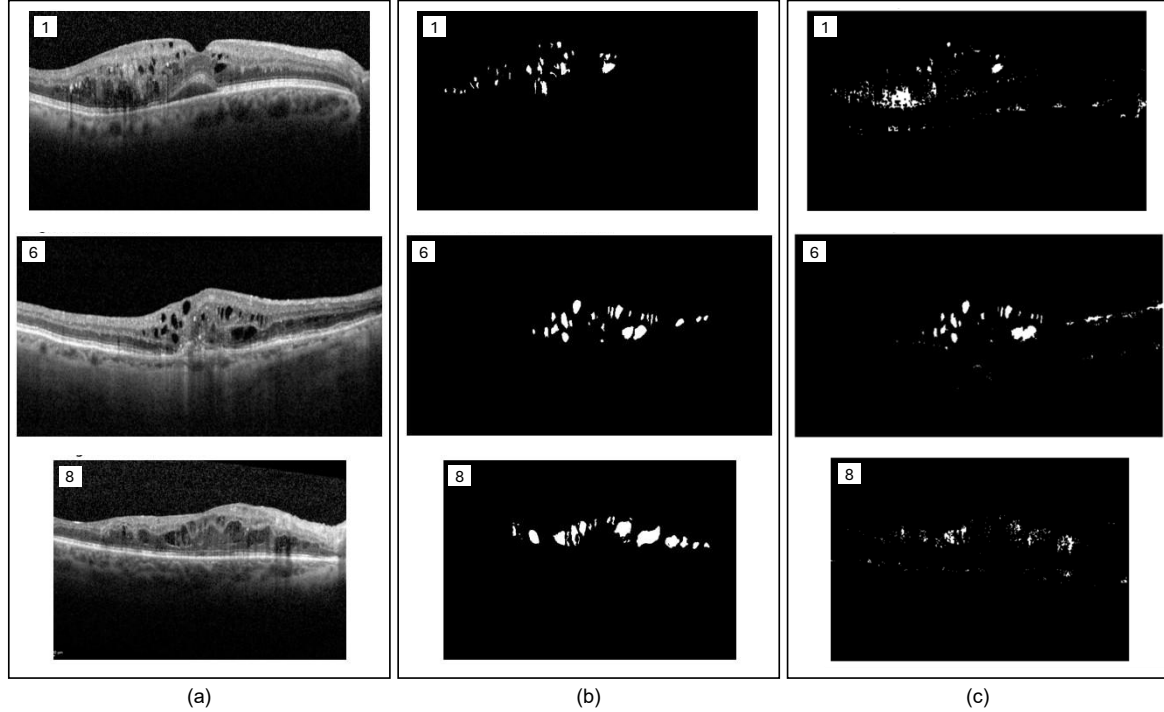


**Figure 6:** Qualitative Segmentation Results. Rows (top to bottom) correspond to Image 1, Image 6, and Image 8. (a) Original OCT image, (b) Ground Truth image, and (c) Predicted Cysts from Proposed Algorithm.

**Table 5:** Comparison of K-means segmentation results with other methods (Manual Threshold and Otsu).

Img	Ground Truth	K-means	Comparison with other methods	
			Manual Threshold	Otsu
1				
3				
6				

In addition, we compared the K-means segmentation approach with other segmentation methods, including Manual Thresholding and Otsu. The results, presented in Table 5, demonstrate a significant difference between the segmentation results obtained by our proposed approach and those obtained by other methods.

## 5 Discussion

Firstly, the primary goal of this work was to develop and evaluate a non-CNN algorithm for segmenting retinal cysts in OCT scans. The proposed algorithm utilised Morphological Operations to define an ROI followed by K-means clustering ( $K = 4$ ) for segmentation, achieved a mean F1 score of 0.492 and a mean mIoU of 0.350. These findings show that the proposed algorithm has better performance compared to an Otsu Thresholding (F1 score: 0.245) and a standard Manual Thresholding (F1 score: 0.458).

Secondly, a key strength of this algorithm is its two-part structure. First, the extensive preprocessing and morphological operations were highly effective at creating an ROI mask that isolated the specific retinal area (between ILM and RPE) by eliminating the noisy background and other non-relevant structures. Second, the K-means algorithm correctly identified the darkest cluster as the cyst class in some images. This approach is qualitatively validated in images such as Image 3 and Image 6 (Table 5), where the predicted segmentation provides clean, accurate, and well-defined cyst structures.

Thirdly, despite the key strength, the algorithm's primary limitation is its sensitivity to noise, resulting in a high rate of false positives (precision: 0.518). This is visually evident in images such as Image 1, Image 4, and Image 9. The K-means algorithm is also a contributing factor because it is a purely intensity-based method that has no concept of shape or connectedness.

In addition, it is also critical to note that the average Accuracy (0.986) is high, this is a misleading metric for this work. This is caused by imbalanced classes because the majority of pixels are background (non-cyst). The mIoU (0.350) and F1 score (0.492) are far more representative metrics for this work, as they appropriately balance precision and recall.

Lastly, the results highlight a trade-off between segmentation quality and computational speed. When maximum quality is the objective, the K-means pipeline is a suitable method, achieving the highest F1 Score and mIoU. However, for real-time applications where speed matters, the Manual Thresholding method offers a better compromise with a comparable F1 Score (0.458). It was  $\pm 13$  times faster than K-means. In contrast, the Otsu thresholding method is not recommended for this task due to its low overall precision (0.142).

## 6 Conclusion

### 6.1 Summary

In this report, we successfully implemented an automated pipeline for segmenting retinal cysts in OCT images. The method, based on Otsu thresholding for ROI generation and K-means clustering for cyst segmentation, achieved a processing time of 0.131 seconds, mIoU score of 0.35, accuracy of 0.986, precision of 0.518, recall of 0.530, and F1 score of 0.492. The main achievement of this proposed algorithm is its robust ROI generation, which effectively eliminates false positives in the regions outside the ILM and RPE. The primary limitation is that modest mIoU and F1 scores indicate that the K-means clustering still struggles to identify retinal cysts.

### 6.2 Future Work

In future work, various preprocessing techniques can be employed to reduce noise in the retina area as part of the data preparation process before segmentation. Additionally, other postprocessing techniques can be utilised to remove objects, except for cysts, based on size, shape, and orientation.

## References

- [1] Gopinath, K. and Sivaswamy, J. (2019). Segmentation of retinal cysts from optical coherence tomography volumes via selective enhancement. *Ieee Journal of Biomedical and Health Informatics*, 23(1), 273-282. <https://doi.org/10.1109/jbhi.2018.2793534>
- [2] Hafeez, F., Suhail, Z., & Zwiggelaar, R. (2023). Morphological and marker-based watershed method for detection and segmentation of brain tumor regions. *Nust Journal of Engineering Sciences*, 16(2), 108-113. <https://doi.org/10.24949/njes.v16i2.759>
- [3] Ravichandran, G., Elangovan, P., & Nath, M. K. (2019). Diagnosis of retinitis pigmentosa from retinal images. *International Journal of Electronics and Telecommunications*, 65(3), 519–525. <https://doi.org/10.24425/ijet.2019.129808>